ARTICLE

BIOTECHNOLOGY and BIOENGINEERING

A Droplet Microfluidics Platform for Rapid Microalgal Growth and Oil Production Analysis

Hyun Soo Kim,[1] Adrian R. Guzman,[1] Hem R. Thapa,[2] Timothy P. Devarenne,[2] Arum Han[1,3]

[1]Department of Electrical and Computer Engineering, Texas A&M University, College Station, Texas

[2]Department of Biochemistry and Biophysics, Texas A&M University, College Station, Texas

[3]Department of Biomedical Engineering, Texas A&M University, College Station, Texas 77843; telephone: +1-979-845-9686; fax: +1-979-845-6259; e-mail: arum.han@ece.tamu.edu

ABSTRACT: Microalgae have emerged as a promising source for producing future renewable biofuels. Developing better microalgal strains with faster growth and higher oil production rates is one of the major routes towards economically viable microalgal biofuel production. In this work, we present a droplet microfluidics-based microalgae analysis platform capable of measuring growth and oil content of various microalgal strains with single-cell resolution in a high-throughput manner. The platform allows for encapsulating a single microalgal cell into a water-in-oil emulsion droplet and tracking the growth and division of the encapsulated cell over time, followed by on-chip oil quantification. The key feature of the developed platform is its capability to fluorescently stain microalgae within microdroplets for oil content quantification. The performance of the developed platform was characterized using the unicellular microalga *Chlamydomonas reinhardtii* and the colonial microalga *Botryococcus braunii*. The application of the platform in quantifying growth and oil accumulation was successfully confirmed using *C. reinhardtii* under different culture conditions, namely nitrogen-replete and nitrogen-limited conditions. These results demonstrate the capability of this platform as a rapid screening tool that can be applied to a wide range of microalgal strains for analyzing growth and oil accumulation characteristics relevant to biofuel strain selection and development.

Biotechnol. Bioeng. 2016;113: 1691–1701.

KEYWORDS: droplet microfluidics; high-throughput analysis; microalgal biofuel; on-chip oil staining; microalgal library screening

Introduction

Microalgae are considered a promising future renewable source of chemicals as they can utilize sunlight and atmospheric CO_2 to produce a variety of biomolecules, including a wide range of oil types for biofuel feedstocks (Chisti, 2007, 2013; Georgianna and Mayfield, 2012; Mata et al., 2010; Pulz and Gross, 2004; Scott et al., 2010; Spolaore et al., 2006). In terms of biofuel feedstocks, compared to current photosynthetic organisms such as corn, soybean, and sugarcane, which are used for the production of first-generation biofuels, microalgae have higher growth rates and oil content, and also do not compete with food production and arable land usage (Chisti, 2007; Mata et al., 2010; Scott et al., 2010). Although these advantages make microalgae-based biofuels more attractive, current production costs are not yet economically competitive, and thus significant improvements in productivity are needed (Chisti, 2013; Georgianna and Mayfield, 2012; Kim et al., 2014). These improvements include developing microalgal strains with higher growth rates and/or oil production, optimizing their culture environment (e.g., light condition or nutrient composition), scaling up to larger cultures, and developing better dewatering and oil extraction methods (Chisti, 2013; Georgianna and Mayfield, 2012; Kim et al., 2014).

Developing highly efficient microalgal strains is the first step towards achieving economically viable microalga-based biofuels, which can be achieved through identification of new strains, genetic and metabolic engineering, or adaptive evolution (Chisti, 2013; Georgianna and Mayfield, 2012). These methods typically involve screening processes where sample cell populations are diluted and cultured on media plates, followed by manually selecting cells that show traits of interest (i.e., enhanced growth and oil production). Although this process is widely utilized, it is labor-intensive, time-consuming, and requires relatively long culture periods. Also, the large number of samples (10^5–10^6) to be analyzed in a typical single screening assay makes this process one of the major bottlenecks in strain development.

Droplet microfluidics-based systems have shown the capability to perform extremely high-throughput assays (Brouzes et al., 2009; Guo et al., 2012; Lagus and Edd, 2013; Teh et al., 2008). In

Hyun Soo Kim and Adrian R. Guzman contributed equally to this work.

Correspondence to: A. Han

Contract grant sponsor: National Science Foundation (NSF) Emerging Frontiers in Research and Innovation (EFRI)

Contract grant number: #1240478

Received 7 October 2015; Revision received 21 December 2015; Accepted 28 December 2015

Accepted manuscript online 1 January 2016;

Article first published online 3 February 2016 in Wiley Online Library (http://onlinelibrary.wiley.com/doi/10.1002/bit.25930/abstract).

DOI 10.1002/bit.25930

such systems, each aqueous droplet suspended in carrier oil through a water-in-oil emulsion process functions as an independent femto-, pico-, or nano-liter volume bioreactor. These droplets, each capable of encapsulating one or more cells, can be individually transported, mixed with each other, and analyzed, allowing for massively parallel processing and experimentation within a short period of time. Droplet microfluidics-based systems have thus been successfully utilized in a variety of screening applications, including drug discovery, synthesis of biomolecules, diagnostics, enzymatic activity investigation, and engineering proteins through directed evolution (Guo et al., 2012; Hua et al., 2010; Jakiela et al., 2013; Mazutis et al., 2009; Ostafe et al., 2014; Pekin et al., 2011; Seiffert and Weitz, 2010; Sjostrom et al., 2014; Teh et al., 2008).

Despite this tremendous potential, only a few droplet microfluidics-based platforms for screening microalgae phenotypes have been reported to date. Droplet generators integrated with downstream culture chambers have been employed to encapsulate single microalgal cells in droplets and monitor these droplets over time for growth profile characterization, but without oil analysis capabilities (Dewan et al., 2012; Pan et al., 2011). Alginate hydrogel-based microcapsules encapsulating a single BODIPY-stained microalgal cell to analyze the heterogeneity of oil accumulation among species and differences in oil accumulation among individual cells within the same species have been demonstrated, but lacks the capability of growth analysis (Lee et al., 2013). Recently, a digital microfluidic system capable of analyzing both microalgal growth and oil production was developed, but this platform is limited in throughput by the number of samples that can be analyzed simultaneously (one microalgal sample per device) (Shih et al., 2014). Also, this platform lacks single-cell level analysis capabilities, which will be crucial in developing microalgal strains with improved traits. In order for droplet microfluidics-based systems to be utilized as a high-throughput screening tool for analyzing large numbers of microalgal strains, the platform needs to have the capabilities of analyzing both growth and oil production at the single-cell level within a single device (i.e., on-chip analysis) seamlessly, something that the previously reported platforms lack.

Here we present a high-throughput droplet microfluidics-based microalgae screening platform capable of analyzing both growth and oil production at the single-cell level, with all steps occurring seamlessly on-chip. Single microalgal cells were encapsulated into droplets and cultured for a period of time for growth profile acquisition, followed by on-chip oil staining and analysis for oil quantification. The main technological innovation of this platform is that the platform allows on-chip staining of microalgal oil by merging the cell-encapsulated droplet with a neutral lipid-staining fluorescent dye (Nile red) droplet one-to-one, as well as overcoming the high fluorescence background caused by Nile red staining of carrier oil through a droplet rinsing process. Thus the presented platform allows, for the first time, the entire process of quantifying microalgal growth and lipid accumulation with single-cell resolution all on a single chip, paving the way towards high-throughput screening. The platform was characterized and demonstrated using a unicellular microalga, *Chlamydomonas reinhardtii*, and a colonial microalga, *Botryococcus braunii*, as a proof of concept analysis.

Materials and Methods

Design of the Droplet Microfluidics-Based Microalgae Analysis Platform

The droplet microfluidics-based microalgae analysis platform is composed of three functional parts; a droplet generation/culturing region, an on-chip droplet staining region, and a droplet rinsing/analysis region (Figs. 1 and 2A). First, in the droplet generation/culturing region, droplets (240 μm in diameter) containing a single cell suspended in culture media were generated using a standard T-junction droplet generator (Guzman et al., 2015; Lagus and Edd, 2013; Teh et al., 2008). The T-junction droplet generator was comprised of a 200 μm wide channel for a continuous oil phase (carrier oil) and a perpendicular 160 μm wide orifice for supplying the microalgae-suspended culture media (Fig. 2B). In this configuration the viscous oil having a higher flow rate shears the culture media solution containing cells to generate droplets (Fig. 2B). The cell-encapsulated droplets were held in a downstream culture chamber to monitor the growth of microalgae inside the same droplets over time. A 200 μm wide serpentine microchannel was designed as the culture chamber, where a microchannel having narrower width compared to the droplet size was utilized to slightly squeeze the droplets. This allowed for maintaining consistent spacing between neighboring droplets that not only provided precise droplet ordering for time-course growth analysis of the same droplet, but also prevented unexpected droplet merging throughout the culturing period (Fig. 2C).

One of the key innovations in the developed platform is the on-chip oil staining capability of cells within droplets. Nile red fluorescent dye that binds to neutral lipids was utilized in the on-chip staining process to quantify oil accumulation in cells (Elsey

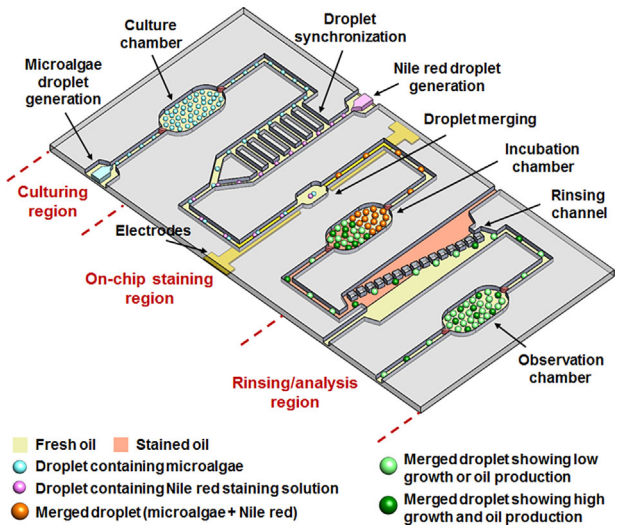

Figure 1. Illustration of the droplet microfluidics-based microalgae screening platform for analyzing microalgal growth and oil production. The platform is composed of three functional parts—the droplet generation/culturing region for culture and growth monitoring, the on-chip staining region for tagging Nile red fluorescent dye to oil bodies of microalgae, and the rinsing/analysis region for oil quantification.

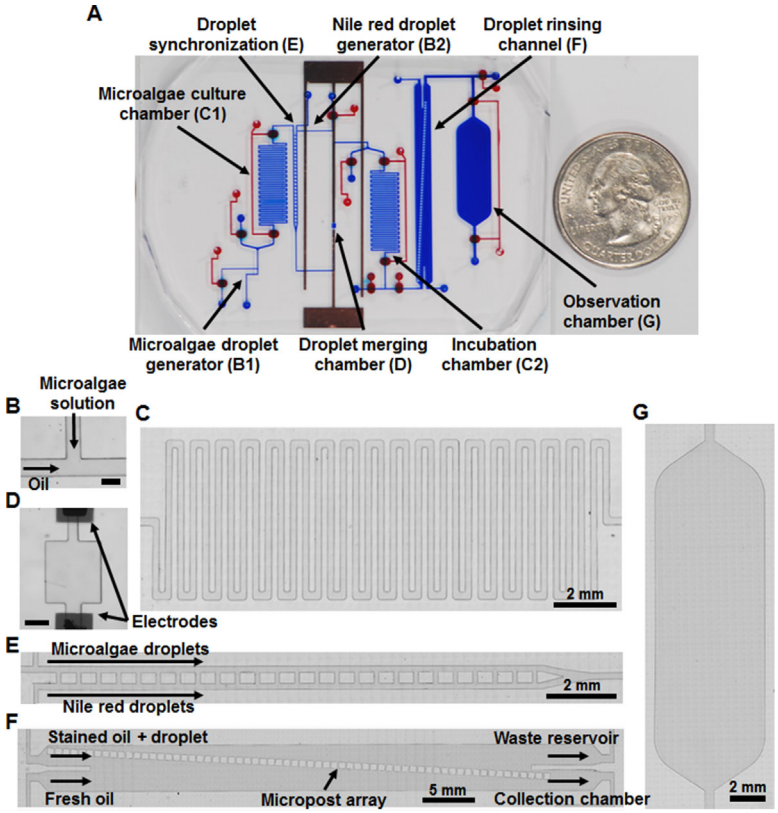

Figure 2. Microfabricated platform. (**A**) Photograph of the assembled device. Micrographs of the (**B**) T-junction droplet generator for producing cell solution and Nile red solution droplets (scale bar = 200 μm), (**C**) culture/incubation chamber, (**D**) on-chip droplet merging chamber (scale bar = 300 μm), (**E**) railroad-like structure to adjust the flow resistance between droplets used for droplet synchronization, (**F**) droplet rinsing region consisting of an angled micropost array (3°), and (**G**) observation chamber.

et al., 2007; Kim et al., 2014). In order to achieve on-chip staining, droplets containing Nile red molecules dissolved in dimethyl sulfoxide (DMSO) (240 μm in diameter) were created using a second T-junction droplet generator in the on-chip staining region. These Nile red droplets were synchronized with the droplets containing microalgae (released from the culture chamber) through a railroad-like structure (Fig. 2E). This railroad-like structure (200 μm wide parallel channels linked by 100 μm wide rails that are spaced 200 μm apart) equalized the fluidic resistance between the two trains of droplets (microalgae-containing droplets and Nile red solution droplets), enabling one-to-one droplet pairing at the end of the synchronization region (Ahn et al., 2011). These synchronized droplets were then merged inside a merging chamber ($500 \times 500\ \mu m^2$) by applying an electric field using two integrated electrodes (Guzman et al., 2015; Lagus and Edd, 2013; Zagnoni et al., 2010), exposing cells inside the droplet to Nile red molecules, which stained oil bodies within the encapsulated cells (Fig. 2D). For complete staining, the merged droplets were stored in a serpentine incubation chamber, that was the same as the culture chamber (Fig. 2C), for 0–10 min.

Due to the innate nature of Nile red molecules diffusing into hydrophobic carrier oil, the carrier oil surrounding the merged droplets was also stained with Nile red during the on-chip staining process, creating severe fluorescence background and preventing adequate fluorescence imaging/detection for lipid quantification. This was resolved by a droplet rinsing process. A droplet rinsing channel having a 3° angled micropost array (size: $400 \times 400\ \mu m^2$) was utilized in the rinsing/analysis region (Fig. 2F). This is similar to a design by (Sochol et al., 2012), where such a structure was used for microbead processing. This micropost array was positioned between two parallel laminar oil flows (fresh carrier oil flow and Nile red strained oil flow) and functioned as a droplet guiding structure, physically transferring the droplets from the Nile red stained carrier oil flow to the fresh carrier oil flow without obstructing oil flow. The rinsed droplets were then collected in an observation chamber (Fig. 2G; $3 \times 10\ mm^2$) and oil production was quantified with fluorescence microscopy.

Microfabrication

The platform was fabricated in poly(dimethylsiloxane) (PDMS) (10:1 mixture) using a typical soft-lithography technique. First, the master molds for the bottom channel layer (height: 160 μm) and the top valve layer (height: 250 μm) were fabricated with SU-8^{TM} photoresist (SU-8 2075, Microchem Inc., MA) on silicon wafers using a conventional photolithography process. The thin PDMS layer (250 μm thick) containing the microfluidic channel was made by spin-coating 4.5 g of PDMS pre-polymer at the speed of 300 rpm

for 40 s, and the thick PDMS valve layer (4 mm thick) was replicated by pouring 24 g of PDMS pre-polymer. The Cr/Cu electrodes (200 and 3000 Å thick, respectively) used to induce on-chip droplet merging were patterned on a $50.8 \times 76.2\,mm^2$ glass slide. A thin PDMS layer (30 μm thick) was then spin-coated on the electrode-patterned glass slide to create a hydrophobic bottom surface (3000 rpm for 40 s). All three layers (the channel layer, the valve layer, and the electrode layer) were aligned and bonded through oxygen plasma treatment. After assembly, the devices were kept at room temperature for at least 2 days to recover the hydrophobic microchannel surface properties necessary for stable droplet generation.

Cell Preparation

Chlamydomonas reinhardtii, strain CC-125, was grown in Tris-acetate-phosphate (TAP) media (Gorman and Levine, 1965; Harris et al., 2009) at 23°C under a light intensity of 80 μmol photons $\cdot m^{-2} \cdot s^{-1}$ with a 12 h light-dark cycle, and was collected in the exponential growth phase. This collected sample was diluted to a concentration of 1.38×10^5 cells/mL to encapsulate a single microalga into a droplet, and used for growth analysis. Oil accumulation was induced in *C. reinhardtii* by culturing in TAP media lacking NH_4Cl (TAP-N) for 4–5 days before use. A solution of these cells with a concentration of 8.85×10^6 cells/mL was prepared and loaded into the platform to encapsulate approximately 64 cells in a single droplet for on-chip Nile red staining characterization.

Botryococcus braunii race B, Berkeley (or Showa) strain (Nonomura, 1988) was cultured in modified Chu 13 media (Grung et al., 1989) at 22.5°C under a light intensity of 80 μmol photons $\cdot m^{-2} \cdot s^{-1}$ with a 12 h light-dark cycle (Kim et al., 2014; Weiss et al., 2010, 2012). The cultures were continuously aerated with filter-sterilized air containing 2.5% CO_2. *B. braunii* colonies in exponential growth phase (6–8 days after subculture) were collected, filtered for colony size selection (diameter of *B. braunii* colonies after filtering: 70–100 μm), and used for on-chip Nile red staining.

Operation of the Droplet Analysis Platform

Droplets were generated in the developed platform using mineral oil (J217 Mineral Oil Light White, Amresco, OH) with surfactant (2% wt/wt, Abil EM90, Evonik, TX) as the carrier oil. Various flow rates of carrier oil, microalgae sample solution, and Nile red solution in DMSO were tested and optimized to obtain one-to-one droplet synchronization of similar diameter droplets (240 μm) between the microalgae solution and the Nile red solution. The condition at which droplet sizes matched and droplets were well paired was found experimentally. Flow rates of microalgae sample solution and carrier oil used for generating droplets containing microalgae were 272 and 55 μL/h, respectively, and flow rates of Nile red solution and carrier oil for Nile red droplets were 180 and 55 μL/h, respectively. When the droplets containing microalgae were released from the culture chamber and reflowed into the on-chip droplet staining region, a flow rate of 327 μL/h (272 + 55 μL/h) was used in the carrier oil. Droplet merging was characterized by applying a 150 V AC signal to induce an electric field in the merging region.

Characterization of Droplet Rinsing

The effect of droplet rinsing (i.e., Nile red stained droplet transfer from stained carrier oil to fresh carrier oil for fluorescence background removal) was characterized by changing the combinations of flow rates between stained oil and fresh oil, followed by conducting fluorescence image analysis (light intensity profile measurement, NIH Image J software) to analyze Nile red molecule diffusion into the fresh oil. Three different stained oil flow rates (225, 450, and 562 μL/h) were selected to flow Nile red stained droplets into the droplet rinsing channel, and five different flow rate ratios between the stained oil flow and the fresh oil flow (1:2, 1:2.5, 1:3, 1:3.5, and 1:4) were compared and used to characterize rinsing efficiency. For example, when a flow rate of 450 μL/h was used for stained oil reflow, flow rates of 900, 1125, 1350, 1575, and 1800 μL/h were used for the fresh oil.

Characterization of On-Chip Nile Red Staining

The capability of oil analysis in the platform was first characterized through on-chip Nile red staining of 64 N-starved *C. reinhardtii* cells in droplets. Various concentrations of Nile red solution (1, 5, 10, 25, and 100 μg/mL in DMSO) as well as incubation times (0, 3, 6, and 10 min) were tested, and staining results were compared to off-chip Nile red stained samples. For the off-chip stained sample (control), 100 μL of *C. reinhardtii* cells suspended in media were treated with 20 μL of Nile red dissolved in DMSO (25 μg/mL) for 10 min, where the actual concentrations of Nile red and DMSO were 5 μg/mL and 20%, respectively. The effect of on-chip Nile red staining was confirmed by measuring the Nile red fluorescence intensity per unit area in *C. reinhardtii* oil bodies, and then comparing the average of these values to that obtained from off-chip stained samples. Microscopy for Nile red fluorescence (excitation: 460–500 nm, emission: 560–600 nm) and chlorophyll autofluorescence (excitation: 460–500 nm, emission >610 nm) were conducted using a Zeiss Axio Observer Z1 microscope (Carl Zeiss Micro Imaging, LLC) equipped with a digital camera (Orca Flash2.8 CMOS Camera), and all microscopic images were analyzed with NIH Image J software.

On-Chip Staining of *B. braunii*

All procedures for both on-chip and off-chip *B. bruanii* oil staining and analysis remained the same as previously described (see "Characterization of on-chip Nile red staining") except for the fixed incubation time (20 min) and emission filter (500–550 nm) for Nile red fluorescence microscopy. Afterwards, the on-chip stained *B. braunii* colonies were also collected to an outlet reservoir for further analysis, where the collected samples were placed between glass slides to examine whether oil content inside individual cells as well as in the extracellular matrix were sufficiently stained.

Analysis of Growth and Oil Accumulation in *C. reinhardtii* Under Different Culture Conditions

To demonstrate the rapid analysis functionality of the developed platform, growth and oil accumulation of *C. reinhardtii* cells under two different culture media conditions (N-replete condition: 100%

nitrogen [TAP media], N-deplete condition: 0% nitrogen [TAP-N media]) were tested on chip. Droplets containing a single *C. reinhardtii* cell suspended in TAP and TAP-N media were generated, respectively. Both cultures were carried out for 6 days under a light intensity of 80 μmol photons $\cdot m^{-2} \cdot s^{-1}$ with a 12 h light-dark cycle. Tracking the same droplets stored in the culture chamber allowed time-course growth analysis, where growth of *C. reinhardtii* was characterized by counting the number of cells inside droplets based on chlorophyll autofluorescence. In addition, oil accumulation in *C. reinhardtii* cells was analyzed over time, which was estimated by measuring the fluorescence intensity per unit area in *C. reinhardtii* through sequential time-course on-chip Nile red staining, fluorescence microscopy, and image analysis (described in "Characterization of on-chip staining in the screening platform" section).

Results

On-Chip Droplet Generation, Synchronization, and Merging

Droplets containing a single microalgal cell (240 μm in diameter) were successfully generated by flowing carrier oil with surfactant and microalgae suspended in culture media at a flow rate of 272 and 55 μL/h, respectively. Cell encapsulation in droplets follows a Poisson distribution that describes the droplet occupancy statistics, and here, ~30% of the generated droplets contained a single cell (Fig. S1) (Clausell-Tormos et al., 2008; Koster et al., 2008). The same size droplets containing Nile red molecules dissolved in DMSO (240 μm in diameter) were produced using a flow rate of 180 μL/h for the oil and 55 μL/h for the Nile red solution (Movie S1). Different carrier oil flow rates were required to obtain the same size droplets due to the very large difference in viscosity between the two solutions (culture media vs. DMSO = 0.886 vs. 1.990 cp at 25°C). These two trains of droplets were then successfully synchronized to a one-to-one pair using the railroad-like pressure equalizing structure (Movie S1). Once the synchronized droplet pairs entered the merging chamber, a square wave (10 kHz) electric pulse of 150 V achieved 95% one-to-one droplet merging efficiency (Movie S2). Occasionally, more than two droplets were merged together or one unmerged droplet passed by the merging chamber, which comprised the remaining 5% of droplets. However, these droplets could be easily recognized and excluded from the growth/oil accumulation analysis due to their vastly different sizes compared to the one-to-one merged droplets.

On-Chip Droplet Rinsing

Utilizing the micropost array structure in the rinsing channel, Nile red stained droplets were successfully transferred from the stained carrier oil flow to the fresh carrier oil flow, both flowing side-by-side under the laminar flow regime (Fig. 3A). The rinsing effect (i.e., removal of fluorescence background) was initially characterized using a stained oil flow rate of 225 μL/h, and then the same characterization was conducted using faster flow rates (450 and 562 μL/h) to test whether the platform can achieve higher throughput. 450 μL/h was chosen to double the lowest flow rate and 562 μL/h was selected to mimic the case where all on-chip procedures after droplet culture (i.e., on-chip Nile red staining, droplet rinsing, and observation processes) can be carried out continuously (i.e., without an incubation step for complete staining) to increase overall system throughput. Fluorescence intensity profile measurements were taken across the rinsing channel (X [left] ~ Y [center] ~ Z [right]) for the inlet, middle, and outlet parts of the rinsing channel to analyze the rinsing effect (Fig. 3A). At a flow rate of 225 μL/h and a fresh oil flow rate of 675 μL/h or higher (i.e., more than three times higher than the flow rate of the droplet-suspended stained oil), the fluorescence intensity profile confirmed that all fluorescence background from the stained oil was removed through the droplet rinsing channel (Fig. 3B). Additionally, Nile red stained droplets were successfully guided into the fresh oil flow under these conditions (Fig. 3C and Movie S3), resulting in no background fluorescence in the observation chamber (Fig. 3D). However, when the flow rate of the fresh oil was less than 560 μL/h (i.e., less than 2.5 times of the stained oil flow rate of 225 μL/h), the stained oil could not be completely flushed out and seeped into the observation chamber (i.e., droplets were not sufficiently rinsed), which resulted in some remaining fluorescence background (Figs. 3E–F, S2, and Movie Video S4). At a stained oil flow rate of 450 μL/h, the same result was observed where a fresh oil flow rate of 1350 μL/h or higher (i.e., more than three times faster than the stained oil flow) completely flushed out the stained oil and successfully transferred the droplets into the fresh oil flow. At a stained oil flow rate of 562 μL/h, the stained droplets were adequately rinsed using a fresh oil flow rate of 1970 μL/h or higher (i.e., more than 3.5 times greater than the stained oil flow rate, Figs. 3F and S2). The effect of this rinsing process is also shown in Figure 3D and E where no fluorescence background was observed after the droplet rinsing process, while severe fluorescence background signal was found without this step or when rinsing was incomplete. In all subsequent experiments, the flow rates of 450 and 1350 μL/h were utilized as the stained and fresh oil flow rates, respectively.

Characterization of On-Chip Stained Microalgal Oil

In order to test the on-chip Nile red staining capability (i.e., Nile red staining of oil within microalgal cells) in the platform, *C. reinhardtii* cultures grown in N-deplete conditions (0% nitrogen) were used since *C. reinhardtii* accumulates triacylglycerol oil bodies under stressed conditions such as nitrogen depletion (Harris et al., 2009; Moellering and Benning, 2010). Droplet encapsulation of 64 N-starved C. *reinhardtii* cells per droplet was conducted to mimic the situation of single-cell encapsulation and culture for 2–3 days (considering 8–12 h of *C. reinhardtii* doubling time, 48–72 h is required to produce 64 cells from a single cell). A 2- or 3-day culture period was selected as that would be the required time to accumulate enough cells for adequate comparison of growth rates among different microalgal strains or mutants. Combinations of five different Nile red concentrations (1, 5, 10, 25, and 100 μg/mL in DMSO) and four different incubation times in the incubation chamber (0, 3, 6, and 10 min) were tested, and their fluorescence intensities were compared to that of the off-chip stained samples (control). At least 100 samples were analyzed ($n = 100$) to obtain the

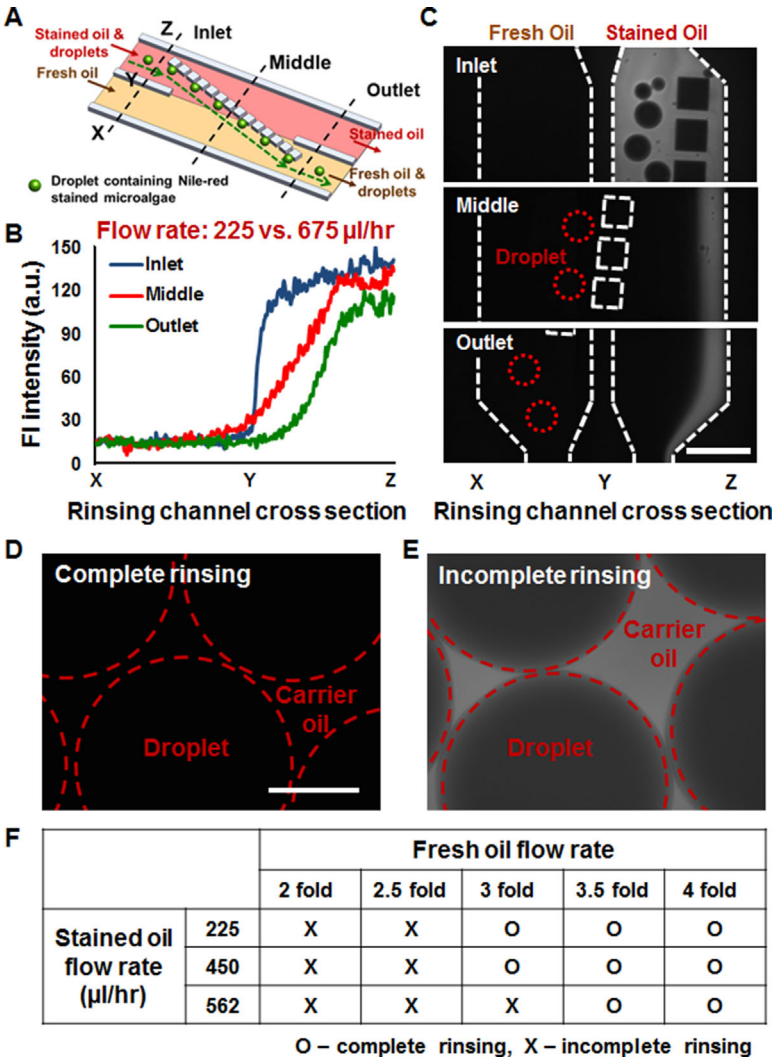

Figure 3. Characterization of the droplet rinsing process. (**A**) Enlarged schematic of the droplet rinsing channel. (**B**) Fluorescence intensity profile through the rinsing channel, which shows the flushing out of the stained oil towards the waste outlet (stained oil: fresh oil = 225 μL/h: 675 μL/h). (**C**) Microscopic images showing the stained oil rinsing process through the rinsing channel—at the inlet, the middle, and the outlet parts of the channel (stained oil: fresh oil = 225 μL/h: 675 μL/h). Scale bar = 600 μm. (**D**) Droplets collected inside the observation chamber after completion of the droplet rinsing process (stained oil: fresh oil = 225 μL/h: 675 μL/h). Scale bar = 150 μm. (**E**) Droplets collected inside the observation chamber when the rinsing process was incomplete (stained oil: fresh oil = 225 μL/h: 560 μL/h). (**F**) Analysis of the rinsing effect when using different flow rates for the stained oil and fresh oil.

average fluorescence intensity value from each condition tested. Figure 4A shows representative images of Nile red stained *C. reinhardtii* cells inside droplets compared to those stained off-chip, where variations in fluorescence intensities could be observed depending on the Nile red concentrations and incubation times used.

At a concentration of 1 μg/mL, Nile red fluorescence intensity of *C. reinhardtii* reached only 92% of the off-chip stained samples even after a 10 min incubation time (Fig. 4B). Assuming that more than 95% of staining similarity is deemed comparable to the off-chip staining, no comparable staining could be achieved at 1 μg/mL Nile red concentration, regardless of the incubation time. When using 5 μg/mL and an incubation time of 3 min or longer, the fluorescent intensity reached greater than 95% of that from the off-chip stained samples (control), thus showing comparable result to off-chip staining (Fig. 4B). Nile red concentrations greater than 10 μg/mL led to staining results comparable to the off-chip stained sample regardless of the incubation time even without any incubation (Fig. 4B). One aspect to note here is that the incubation time defined here does not include the time required for the Nile red merged droplets to flow through the rinsing channel and move into the observation chamber, which takes ~1.5 min. So even in the case defined as zero incubation time that does not involve any additional post-merging on-chip incubation step, there was still 1.5 min of time where Nile red molecules could stain lipid bodies in *C. reinhardtii* cells before being analyzed. As introducing the on-chip incubation steps (i.e., waiting time) lowers the overall throughput, Nile red concentration of 10 μg/mL or higher was used in all subsequent experiments to eliminate the incubation step.

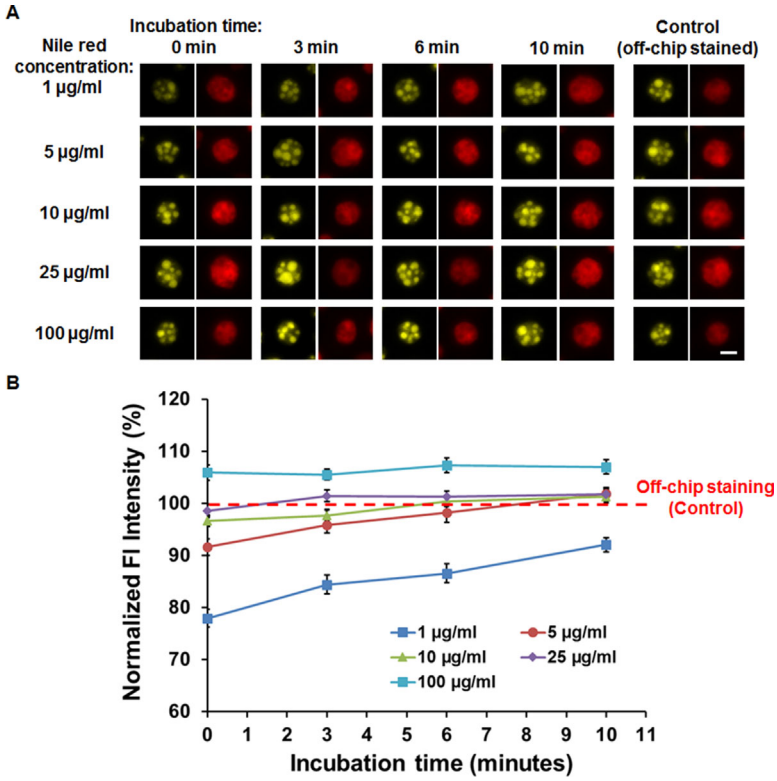

Figure 4. Characterization of the on-chip Nile red staining process. (**A**) Nile red stained oil bodies (yellow) in *C. reinhardtii* cells showing different fluorescence intensities when using different Nile red concentrations and incubation time. Red color indicates chlorophyll autofluorescence of the *C. reinhardtii* cells. (**B**) Analysis of average fluorescence intensities of oil bodies stained with different concentrations of Nile red dye and incubation time ($n = 100$) normalized to off-chip stained samples (control). All data shown are mean ± standard error. Scale bar = 5 µm.

Analysis of *C. reinhardtii* Growth and Oil Accumulation Under Different Culture Conditions

C. reinhardtii cells in the droplet screening platform were grown for 6 days under two different culture conditions (i.e., N-replete [100% nitrogen] and N-deplete [0% nitrogen]) to investigate and compare the growth and oil accumulation under each growth condition (i.e., for validating the capability of the platform to quantify growth and oil production). Time-lapse microscopy showed different growth of *C. reinhardtii* cells resulting from the two different culture conditions (Fig. 5A and Movie Video S5 and S6). Time-course analysis of Nile red stained *C. reinhardtii* cells also showed differences in oil accumulation under the two different culture conditions (Fig. 5B). In order to obtain growth and oil data for both culture conditions (Fig. 5C and D), at least 12 different samples were analyzed for each case ($n = 12$).

In the N-replete condition, the average number of cells inside droplets increased exponentially up to 3 days of culture (day 3), and then the growth slowed down and started to saturate (Fig. 5C), presumably due to nutrient limitation over time. Doubling time of 8–12 h was observed inside the droplets between days 0 and 3, which matches well with previous reports from off-chip observation (Kim et al., 2015; Lee do and Fiehn, 2008). In the N-deplete condition, an increase in the cell population inside the droplets was only observed during the first day of culture (day 1), but then these cells stopped growing as a result of the lack of nutrients (N source) in the culture media (Fig. 5C).

Oil accumulation became higher as *C. reinhardtii* cells were exposed longer to the N starvation condition, while no oil was accumulated in the N-replete condition (Fig. 5D). As Nile-red staining, even at relatively low concentrations, could have potential negative effects on cell behaviors, multiple devices (≥7 devices) were used and each device was sacrificed to conduct the time-course oil accumulation analysis. A maximum increase in oil accumulation under the N-deplete conditions was reached after 4 days of culture, followed by a subsequent decline at days 5 and 6, likely due to the use of the accumulated triacylglycerols as an energy source. This trend showing the oil accumulation inside droplets corresponds well with a recent report where maximum oil accumulation was studied after 3–4 days of N starvation (Cakmak et al., 2012). Compared to *C. reinhardtii* cells cultured in the N-replete condition, an increase in cell size (~100–110% increase, Fig. S3) was observed from the cells in the N-deplete condition (Fig. 5B), which was also a consequence of N starvation (Cakmak et al., 2012).

Oil Quantification in the Colony-Forming Microalga, *B. braunii*

To demonstrate the applicability of the on-chip Nile red staining function for microalgae with different growth habits compared to

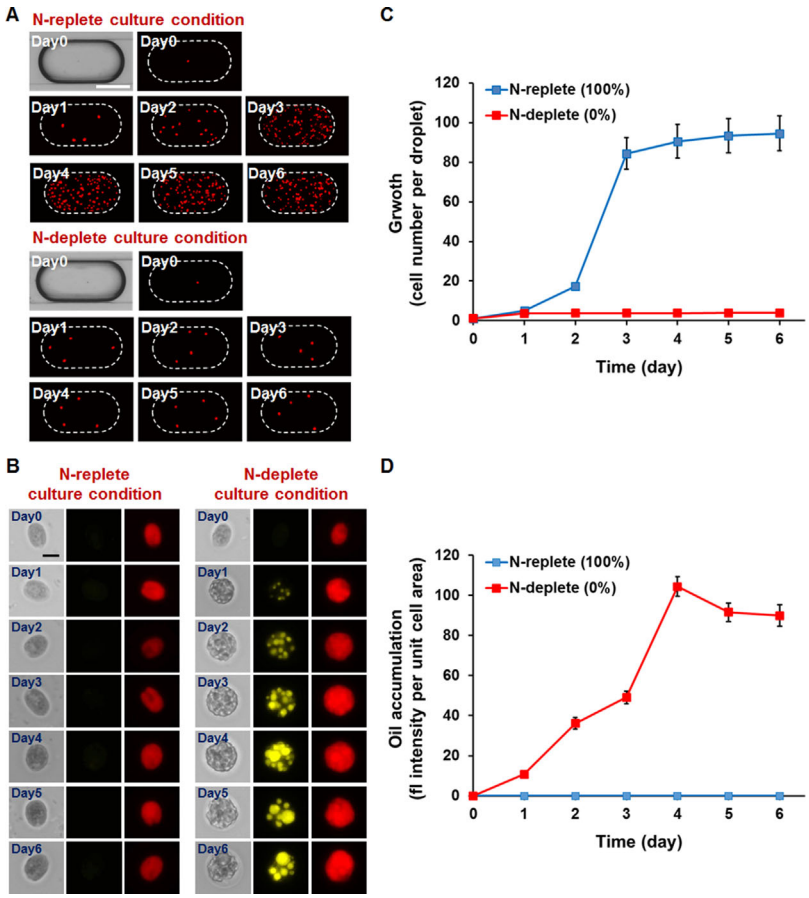

Figure 5. Analysis of growth and oil accumulation in *C. reinhardtii* cells under different culture conditions (N-replete and N-deplete). Time-lapse microscopy showing different (**A**) growth and (**B**) oil accumulation of *C. reinhardtii* cells under N-replete and N-deplete culture conditions. Scale bar: A = 150 μm, B = 5 μm. (**C**) Average number of *C. reinhardtii* cells inside a droplet analyzed for 6 days of culture under N-replete and N-deplete conditions ($n = 12$). (**D**) Average fluorescence intensity of Nile red stained *C. reinhardtii* cells inside a droplet analyzed for 6 days of culture under N-replete and N-deplete conditions ($n = 25$). All data shown are mean ± standard error.

the unicellular *C. reinhardtii*, on-chip staining and analysis of the colony-forming microalga *B. bruanii* was also demonstrated. The B race of *B. braunii* used in this study constitutively accumulates liquid hydrocarbon oil in the range of 30–50% of dry weight, of which 90–95% are retained in the colony extracellular matrix, while the remaining is found in intracellular oil bodies (Banerjee et al., 2002; Weiss et al., 2010). *B. braunii* colonies used in the platform are typically composed of 100–200 individual cells. Due to the larger number of cells as well as higher amount of oil to be stained compared to *C. reinhardtii*, higher concentrations of Nile red solution and a longer incubation (staining) time were required. Among various on-chip Nile red staining conditions tested, a concentration of 2500 μg/mL Nile red solution with an incubation time of 20 min was found to successfully stain both extracellular and intracellular oil contents with a fluorescence intensity comparable to the off-chip stained samples (control) (Fig. 6A and B). At least 25 different samples were analyzed to obtain the average fluorescence intensity value for the control and the optimized conditions ($n = 25$). In order to verify whether the oil content inside individual cells and the extracellular matrix was sufficiently stained, on-chip stained *B. braunii* colonies were collected to an off-chip reservoir and placed between two glass slides. The gentle pressure applied to the glass slides squeezed the 3D shaped *B. braunii* colonies to spread and form a 2D-like planar structure, allowing for examining all individual cells as well as the extracellular matrix. As shown in Figure 6C and D, staining of the oil content in both individual cells and extracellular matrix is comparable to the off-chip stained samples under the above optimized condition.

Discussion

We have for the first time demonstrated a high-throughput droplet microfluidics-based microalgae analysis platform that is capable of analyzing both growth and oil accumulation in microalgae with single-cell resolution. The innovative on-chip staining process within droplets allowed for quantifying microalgal oil content together with growth characterization, overcoming the limitations of previously reported droplet-based microalgae screening systems. In addition, successful analysis and comparison of *C. reinhardtii* cells under different culture conditions validated the capability of the developed platform to be utilized as a high-throughput screening tool for microalgal strain studies.

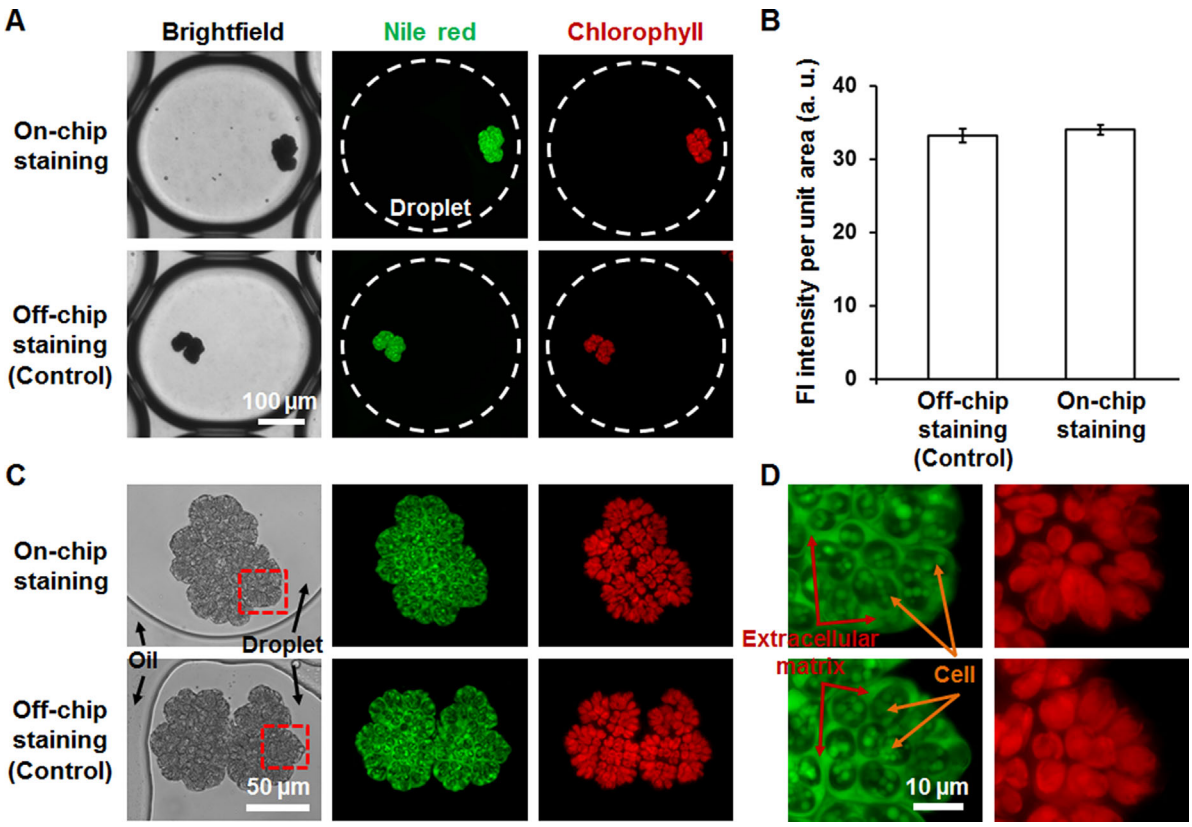

Figure 6. Comparison of on-chip Nile red stained and off-chip Nile red stained *B. braunii*. (**A**) Fluorescence microscopy images showing the on-chip stained *B. braunii* inside droplets compared to those stained off-chip and then encapsulated inside droplets. (**B**) Analysis of average fluorescence intensities from the on-chip staining and the off-chip staining ($n = 25$), which shows around 102% similarity (more than 95% compared to the control). (**C**) Observation of both on-chip and off-chip stained *B. braunii* colonies placed between glass slides to verify sufficient staining of oil content inside individual cells as well as the extracellular matrix. (**D**) Enlarged microscopic images of both on-chip and off-chip stained *B. braunii* from the region highlighted with red dashed square in (**C**). All data shown are mean ± standard error.

In traditional microalgal mutant library screening, both natural and induced, cell populations are diluted and plated on media plates. Colonies showing the desired traits (e.g., faster growth or higher oil production) are identified through microscopy (visual inspection), and then picked, regrown, and tested for trait confirmation. Although this conventional screening and selection process is useful, it is very labor-intensive and its throughput in terms of colony numbers that can be analyzed is low mainly due to manual intervention. To overcome these limitations, we have previously developed a microfluidics-based microalgae screening and selection platform capable of investigating both microalgal growth and oil production with single-cell resolution, followed by selectively extracting cells of interest to off-chip reservoirs for further study (Kim et al., 2015). This microfluidics-based platform was successfully utilized in characterizing growth and oil accumulation of single *C. reinhardtii* cells, and particular *C. reinhardtii* cells were selectively retrieved off-chip afterwards. Although this platform successfully reduced the amount of labor required, its throughput is somewhat limited (∼several thousand samples per platform) considering the large number of samples (10^5–10^6) needed in a typical single screening assay. In order to achieve much higher throughput, a droplet microfluidics-based analysis platform has been developed here. By generating large numbers of uniform-sized droplets within a short period of time, which function as independent bioreactors, this droplet-based platform can carry out massive experiments simultaneously, providing very high-throughput analysis capability. For example, droplet generation as fast as 3.69×10^5 events/s has been reported with very high uniformity (Bardin et al., 2013). In spite of the high-throughput analysis capability, one of the limitations in the droplet microfluidics-based system is that since this system creates closed bioreactors where nutrient and waste exchanges are restricted, long-term culture is challenging. However, in the case of screening assays which require only short culturing periods (e.g., less than 5–7 days), such as microalgal mutant library screening, this droplet-microfluidics based analysis platform will still be desirable. The droplet-based closed bioreactor is also beneficial particularly when using screening assays with motile cells such as *C. reinhardtii* cells. In such cases, the droplets function as a physical barrier that confines motile cells as well as their daughter cells inside, allowing not only for isolating and tracking each motile sample, but also for preventing cross-contamination between different motile cell samples. In addition, the quantitative microscopic fluorescence measurements used in the developed platform will be more accurate than the visual inspection done on plates.

In the present study, oil analysis in the developed platform was designed as an end-point measurement, where cell viability after Nile red staining as well as toxicity from DMSO was not a concern. Rather, achieving the same Nile red staining efficiency through the on-chip staining process compared to the off-chip staining was the main focus. However, it has been reported that high amounts of DMSO are toxic to cells (Velmurugan et al., 2013), and thus cell viability under various DMSO concentrations (50, 2.5, 1, and 0% DMSO after droplet merging) were compared. Droplets containing a single *C. reinhardtii* cell were merged with droplets having 100, 5, 2, and 0% DMSO, and then cell growth was monitored for 3 days under a light intensity of 80 μmol photons $\cdot m^{-2} \cdot s^{-1}$ with a 12 h light-dark cycle. Under 50, 2.5, 1, and 0% DMSO, 0, 74, 86, and 90% of single cells inside the droplets showed viability and growth, respectively. Single *C. reinhardtii* cells in 1 and 0% DMSO droplets showed a similar growth profile, while *C. reinhardtii* cells in 2.5% DMSO droplets displayed a slower growth rate, probably due to recovery form the higher amount of DMSO (Fig. S4). For testing staining efficiency, only the amount of DMSO was changed while maintaining the amount of Nile red molecules (concentration: 5 μg/mL) and the incubation time (10 min) the same for four different cases (i.e., 50, 20, 2.5, and 1% DMSO after droplet merging). As shown in Figure S5, compared to 50% DMSO, 20% DMSO had almost the same staining efficiency of 99%, while 2.5 and 1% DMSO resulted in 79 and 63% staining efficiency, respectively. At lower DMSO concentrations (e.g., 2.5 and 1%), *C. reinhardtii* cells showed growth after on-chip staining even though their staining efficiencies were less effective than higher DMSO concentrations. To increase the staining efficiency using lower DMSO concentrations, further characterization will be required for optimizing the amount of Nile red molecules as well as the incubation time.

After analyzing the growth and oil production of microalgae, droplets containing microalgae showing enhanced growth or oil production can be selectively collected for further analysis. Various droplet sorting techniques based on either an electric field or pneumatic pressure-based actuation are widely utilized to isolate particular droplets of interest (Baret et al., 2009; Cao et al., 2013; Lagus and Edd, 2013). For example, in the electric field based droplet sorting, an applied electric field can deflect particular droplets of interest out of a large number of samples and move only these droplets into a collection chamber. We are currently utilizing such droplet sorting schemes on microalgal mutant libraries to identify and select strains that show faster growth and/or higher oil production.

Successful staining of two different microalgal species, *C. reinhardtii* and *B. braunii*, showed the capability of the developed on-chip staining function which should be applicable to a broad range of microalgae since the droplet size and platform design can be easily adjusted to match any cell shape and size. Cyanobacteria would be a good example, which can be potentially characterized through the developed droplet-based platform. Cyanobacteria are photosynthetic prokaryotes that have been engineered to produce a variety of biofuel related compounds such as ethanol, isobutanol, isoprene, and sesquiterpenes (Atsumi et al., 2009; Davies et al., 2014; Gao et al., 2012; Lindberg et al., 2010; Machado and Atsumi, 2012; Parmar et al., 2011; Savakis and Hellingwerf, 2015). These microorganisms are also advantageous for industrial applications due to their fast growth, simple nutrient requirements, and their genetic tractability (i.e., cyanobacteria are naturally transformable, and thus more amenable to metabolic engineering than other eukaryotic microalgae) (Machado and Atsumi, 2012; Nozzi et al., 2013; Savakis and Hellingwerf, 2015). However, the use of cyanobacteria to produce biofuel-related products is still in early development stages, and further improvements through genetic and metabolic engineering are required. To accomplish this the droplet microfluidics-based analysis platform could be applied, where analysis of both growth and biomolecule production in mutagenized cyanobacteria cell populations will enable the development of better-performing strains with higher productivity, the ability of cells to produce more diverse biofuel products, and would provide new insights into cyanobacterial biology including metabolic pathways and photosynthetic efficiency.

Conclusion

A high-throughput droplet microfluidics-based microalgae analysis platform was developed that enabled for the first time investigation of both growth and oil production of two microalgal species with single-cell resolution. Microalgal growth was characterized by creating independent bioreactors through droplet encapsulation, which allowed for isolated culture of a single microalgal cell as well as monitoring its behavior over time. Oil production in the cells was quantified through the on-chip Nile red staining process, followed by the droplet rinsing process, which are the key features of the developed platform. The capability of on-chip staining for various microalgal strains was successfully validated using the unicellular microalga *C. reinhardtii* and the colonial microalga *B. braunii*. Also, growth and oil accumulation of *C. reinhardtii* under different culture conditions were successfully analyzed and compared, demonstrating the potential screening capability of the platform. We expect that this system will serve as a powerful high-throughput analysis and screening tool to investigate large numbers of microalgal strains at significantly lower costs and reduced time.

This work was supported by the National Science Foundation (NSF) Emerging Frontiers in Research and Innovation (EFRI) grant #1240478 to A.H. and T.P.D. Any opinions, findings, and conclusions or recommendations expressed in this material are those of the author(s) and do not necessarily reflect the views of the National Science Foundation.

References

Ahn B, Lee K, Lee H, Panchapakesan R, Oh KW. 2011. Parallel synchronization of two trains of droplets using a railroad-like channel network. Lab Chip 11(23): 3956–3962.

Atsumi S, Higashide W, Liao JC. 2009. Direct photosynthetic recycling of carbon dioxide to isobutyraldehyde. Nat Biotechnol 27(12):1177–1180.

Banerjee A, Sharma R, Chisti Y, Banerjee U. 2002. Botryococcus braunii: A renewable source of hydrocarbons and other chemicals. Crit Rev Biotechnol 22(3): 245–279.

Bardin D, Kendall MR, Dayton PA, Lee AP. 2013. Parallel generation of uniform fine droplets at hundreds of kilohertz in a flow-focusing module. Biomicrofluidics 7(3):034112.

Baret JC, Miller OJ, Taly V, Ryckelynck M, El-Harrak A, Frenz L, Rick C, Samuels ML, Hutchison JB, Agresti JJ, Link DR, Weitz DA, Griffiths AD. 2009. Fluorescence-activated droplet sorting (FADS): Efficient microfluidic cell sorting based on enzymatic activity. Lab Chip 9(13):1850–1858.

Brouzes E, Medkova M, Savenelli N, Marran D, Twardowski M, Hutchison JB, Rothberg JM, Link DR, Perrimon N, Samuels ML. 2009. Droplet microfluidic technology for single-cell high-throughput screening. Proc Natl Acad Sci USA 106(34):14195–14200.

Cakmak T, Angun P, Demiray YE, Ozkan AD, Elibol Z, Tekinay T. 2012. Differential effects of nitrogen and sulfur deprivation on growth and biodiesel feedstock production of Chlamydomonas reinhardtii. Biotechnol Bioeng 109(8):1947–1957.

Cao Z, Chen F, Bao N, He H, Xu P, Jana S, Jung S, Lian H, Lu C. 2013. Droplet sorting based on the number of encapsulated particles using a solenoid valve. Lab Chip 13(1):171–178.

Chisti Y. 2007. Biodiesel from microalgae. Biotechnol Adv 25(3):294–306.

Chisti Y. 2013. Constraints to commercialization of algal fuels. J Biotechnol 167(3):201–214.

Clausell-Tormos J, Lieber D, Baret JC, El-Harrak A, Miller OJ, Frenz L, Blouwolff J, Humphry KJ, Koster S, Duan H, Holtze C, Weitz DA, Griffiths AD, Merten CA. 2008. Droplet-based microfluidic platforms for the encapsulation and screening of Mammalian cells and multicellular organisms. Chem Biol 15(5):427–437.

Davies FK, Work VH, Beliaev AS, Posewitz MC. 2014. Engineering limonene and bisabolene production in wild type and a glycogen-deficient mutant of synechococcus sp PCC 7002. Front Bioeng Biotechnol 2:21.

Dewan A, Kim J, McLean RH, Vanapalli SA, Karim MN. 2012. Growth kinetics of microalgae in microfluidic static droplet arrays. Biotechnol Bioeng 109(12): 2987–2996.

Elsey D, Jameson D, Raleigh B, Cooney MJ. 2007. Fluorescent measurement of microalgal neutral lipids. J Microbiol Methods 68(3):639–642.

Gao Z, Zhao H, Li Z, Tan X, Lu X. 2012. Photosynthetic production of ethanol from carbon dioxide in genetically engineered cyanobacteria. Energy Environ Sci 5(12):9857.

Georgianna DR, Mayfield SP. 2012. Exploiting diversity and synthetic biology for the production of algal biofuels. Nature 488(7411):329–335.

Gorman DS, Levine RP. 1965. Cytochrome f and plastocyanin: Their sequence in the photosynthetic electron transport chain of Chlamydomonas reinhardtii. Proc Natl Acad Sci USA 54:1665–1669.

Grung M, Metzger P, Liaaen-jensen S. 1989. Primary and secondary carotenoids in two races of the green alga *Botryococcus braunii*. Biochem Syst Ecol 17(4): 263–269.

Guo MT, Rotem A, Heyman JA, Weitz DA. 2012. Droplet microfluidics for high-throughput biological assays. Lab Chip 12(12):2146–2155.

Guzman AR, Kim HS, de Figueiredo P, Han A. 2015. A three-dimensional electrode for highly efficient electrocoalescence-based droplet merging. Biomed Microdevices 17(2):35.

Harris EH, Stern DB, Witman GB. 2009. The Chlamydomonas Sourcebook (Second Edition). Amsterdam: Elsevier. 2000 p.

Hua Z, Rouse JL, Eckhardt AE, Srinivasan V, Pamula VK, Schell WA, Benton JL, Mitchell TG, Pollack MG. 2010. Multiplexed real-time polymerase chain reaction on a digital microfluidic platform. Anal Chem 82(6):2310–2316.

Jakiela S, Kaminski TS, Cybulski O, Weibel DB, Garstecki P. 2013. Bacterial growth and adaptation in microdroplet chemostats. Angew Chem Int Ed Engl 52(34):8908–8011.

Kim HS, Devarenne TP, Han A. 2015. A high-throughput microfluidic single-cell screening platform capable of selective cell extraction. Lab Chip 15(11):2467–2475.

Kim HS, Weiss TL, Thapa HR, Devarenne TP, Han A. 2014. A microfluidic photobioreactor array demonstrating high-throughput screening for microalgal oil production. Lab Chip 14(8):1415–1425.

Koster S, Angile FE, Duan H, Agresti JJ, Wintner A, Schmitz C, Rowat AC, Merten CA, Pisignano D, Griffiths AD, Weitz DA. 2008. Drop-based microfluidic devices for encapsulation of single cells. Lab Chip 8(7):1110–1115.

Lagus TP, Edd JF. 2013. A review of the theory, methods and recent applications of high-throughput single-cell droplet microfluidics. J Phys D Appl Phys 46(11):114005.

Lee DH, Bae CY, Han JI, Park JK. 2013. In situ analysis of heterogeneity in the lipid content of single green microalgae in alginate hydrogel microcapsules. Anal Chem 85(18):8749–8756.

Lee do Y, Fiehn O. 2008. High quality metabolomic data for Chlamydomonas reinhardtii. Plant Methods 4:7.

Lindberg P, Park S, Melis A. 2010. Engineering a platform for photosynthetic isoprene production in cyanobacteria, using Synechocystis as the model organism. Metab Eng 12(1):70–79.

Machado IM, Atsumi S. 2012. Cyanobacterial biofuel production. J Biotechnol 162(1):50–56.

Mata TM, Martins AA, Caetano NS. 2010. Microalgae for biodiesel production and other applications: A review. Renew Sust Energ Rev 14(1):217–232.

Mazutis L, Baret JC, Treacy P, Skhiri Y, Araghi AF, Ryckelynck M, Taly V, Griffiths AD. 2009. Multi-step microfluidic droplet processing: Kinetic analysis of an in vitro translated enzyme. Lab Chip 9(20):2902–2908.

Moellering ER, Benning C. 2010. RNA interference silencing of a major lipid droplet protein affects lipid droplet size in Chlamydomonas reinhardtii. Eukaryot Cell 9(1):97–106.

Nonomura AM. 1988. Botryococcus braunii var. showa (Chlorophyceae) from Berkeley, California United States of America. Jpn J Phycol 36:285–291.

Nozzi NE, Oliver JW, Atsumi S. 2013. Cyanobacteria as a platform for biofuel production. Front Bioeng Biotechnol 1:7.

Ostafe R, Prodanovic R, Lloyd Ung W, Weitz DA, Fischer R. 2014. A high-throughput cellulase screening system based on droplet microfluidics. Biomicrofluidics 8(4):041102.

Pan J, Stephenson AL, Kazamia E, Huck WT, Dennis JS, Smith AG, Abell C. 2011. Quantitative tracking of the growth of individual algal cells in microdroplet compartments. Integr Biol (Camb) 3(10):1043–1051.

Parmar A, Singh NK, Pandey A, Gnansounou E, Madamwar D. 2011. Cyanobacteria and microalgae: A positive prospect for biofuels. Bioresour Technol 102(22): 10163–10172.

Pekin D, Skhiri Y, Baret JC, Le Corre D, Mazutis L, Salem CB, Millot F, El Harrak A, Hutchison JB, Larson JW, Link DR, Laurent-Puig P, Griffiths AD, Taly V. 2011. Quantitative and sensitive detection of rare mutations using droplet-based microfluidics. Lab Chip 11(13):2156–2166.

Pulz O, Gross W. 2004. Valuable products from biotechnology of microalgae. Appl Microbiol Biotechnol 65(6):635–648.

Savakis P, Hellingwerf KJ. 2015. Engineering cyanobacteria for direct biofuel production from CO2. Curr Opin Biotechnol 33:8–14.

Scott SA, Davey MP, Dennis JS, Horst I, Howe CJ, Lea-Smith DJ, Smith AG. 2010. Biodiesel from algae: Challenges and prospects. Curr Opin Biotechnol 21(3): 277–286.

Seiffert S, Weitz DA. 2010. Controlled fabrication of polymer microgels by polymer-analogous gelation in droplet microfluidics. Soft Matter 6(14):3184.

Shih SCC, Mufti NS, Chamberlain MD, Kim J, Wheeler AR. 2014. A droplet-based screen for wavelength-dependent lipid production in algae. Energy Environ Sci 7(7):2366.

Sjostrom SL, Bai Y, Huang M, Liu Z, Nielsen J, Joensson HN, Andersson Svahn H. 2014. High-throughput screening for industrial enzyme production hosts by droplet microfluidics. Lab Chip 14(4):806–813.

Sochol RD, Li S, Lee LP, Lin L. 2012. Continuous flow multi-stage microfluidic reactors via hydrodynamic microparticle railing. Lab Chip 12(20):4168–4177.

Spolaore P, Joannis-Cassan C, Duran E, Isambert A. 2006. Commercial applications of microalgae. J Biosci Bioeng 101(2):87–96.

Teh SY, Lin R, Hung LH, Lee AP. 2008. Droplet microfluidics. Lab Chip 8(2):198–220.

Velmurugan N, Sung M, Yim SS, Park MS, Yang JW, Jeong KJ. 2013. Evaluation of intracellular lipid bodies in Chlamydomonas reinhardtii strains by flow cytometry. Bioresour Technol 138:30–37.

Weiss TL, Chun HJ, Okada S, Vitha S, Holzenburg A, Laane J, Devarenne TP. 2010. Raman spectroscopy analysis of botryococcene hydrocarbons from the green microalga Botryococcus braunii. J Biol Chem 285(42):32458–32466.

Weiss TL, Roth R, Goodson C, Vitha S, Black I, Azadi P, Rusch J, Holzenburg A, Devarenne TP, Goodenough U. 2012. Colony organization in the green alga Botryococcus braunii (Race B) is specified by a complex extracellular matrix. Eukaryotic cell 11(12):1424–1440.

Zagnoni M, Le Lain G, Cooper JM. 2010. Electrocoalescence mechanisms of microdroplets using localized electric fields in microfluidic channels. Langmuir 26(18):14443–14449.

Supporting Information

Additional supporting information may be found in the online version of this article at the publisher's web-site.